METASOMATIC ALTERATION OF THE ALLENDE CAIs: MINERALOGY, PETROGRAPHY, AND OXYGEN ISOTOPIC COMPOSITIONS. A. N. Krot[1*], K. Nagashima[1], M. I. Petaev[2], and G. Libourel[3] [1]University of Hawai'i, USA, *sasha@higp.hawaii.edu; [2]Harvard University, USA; [3]Observatoire de la Côte d'Azur, Nice, France

Introduction: CV (Vigarano type) carbonaceous chondrites experienced high-temperature metasomatic alteration that affected all their major components – refractory inclusions, chondrules, and matrix [1]. Although it is generally accepted that the alteration of chondrules and matrices occurred on the CV parent asteroid, there is still no agreement on the timing (early *vs.* late) and location (nebula *vs.* asteroid) of alteration of refractory inclusions [2–5]. Here we report on the mineralogy, petrography, and *in situ* measured O-isotope compositions of secondary minerals in coarse-grained igneous CAIs [Compact Type A (*TS68*), Type B1 (*AJEF*, *TS21*, *TS23*, *TS34*), B2 (*TS31*), forsterite-bearing Type B (*Al-2* and *Al-5-1*), and Type C (*100* and *160*) from Allende (CV3.6) using the UH Cameca ims-1280 and matrix-matched standards [6].

Mineralogy and Petrography: Coarse-grained igneous CAIs in Allende (CTA, Type B, FoB, and C) consist mainly of spinel, melilite, Al,Ti-diopside, anorthite, and forsterite (only in FoB); perovskite is accessory. Bulk chemical compositions and relative abundances of the major minerals, as well as gehlenite content of melilite vary between different CAI types [7]. Metasomatic alteration of the Allende CAIs affected mainly their primary melilite and anorthite, and, as described below, resulted in formation of different secondary mineral assemblages.

Replacement of melilite and anorthite: Åkermanitic melilite in cores of the Type B1 CAIs *TS21*, *TS23*, *AJEF*, and *TS34* is replaced mainly by grossular and monticellite; forsterite, wollastonite, wadalite, and Na-rich (up 7 wt%), Mg-poor (<1 wt%) melilite are minor (Fig. 1a). The secondary melilite occurs mainly along grain boundaries between altered melilite regions and primary anorthite. The anorthite grains are crosscut by veins of grossular, Ti-free Al-diopside or kushiroite, and Na-melilite.

Highly åkermanitic melilite in FoB CAIs *Al-2* and *Al-5-1* and Type B2 CAI *TS31* is replaced mainly by grossular, wollastonite, and monticellite; Ti-free Al-diopside, wadalite, and Na-rich, Mg-poor melilite are minor. The secondary melilite occurs along grain boundaries with the primary anorthite (Fig. 1b). In *TS31*, these mineral assemblages are crosscut by wollastonite veins (Fig. 1b).

In Type C CAIs *100* and *160*, lacy melilite grains (melilite containing numerous rounded inclusions of anorthite) are pseudomorphically replaced by porous assemblages of grossular, forsterite, and minor monticellite, Ti-free Al-diopside, and Na-rich melilite, which occurs along grain boundaries with primary anorthite (Fig. 1c). In some regions, anorthite is crosscut by grossular veins.

Gehlenitic melilite in the CTA CAI *TS68* and mantles of the Type B1 CAIs is replaced by lath- and needle-shaped anorthite and dmisteinbergite, and grossular. The melilite is also crosscut by numerous veins composed of Mg-bearing (2–3 wt% MgO) grossular, anorthite, and Ti-free Al-diopside. In the veins, (grossular+Al-diopside)/(anorthite+dmisteinbergite) ratio increases towards the CAI cores, which corresponds to increase of åkermanite content of the primary melilite. Melilite and anorthite (primary and secondary), and dmisteinbergite in the peripheral portions of CTA and Type B CAIs are replaced by sodalite, nepheline, and ferroan olivine; the sodalite/nepheline ratio decreases towards the CAI edges.

In Type B1 CAIs, there is a zoned distribution of secondary Na- and Cl-bearing minerals: Na-rich melilite and wadalite occur almost exclusively in the CAI cores, whereas sodalite and nepheline in the CAI peripheries.

Secondary minerals in voids and cracks: All types of Allende CAIs studied contain voids and cracks, which are often filled by subhedral grains of wollastonite, hedenbergite, andradite, grossular, monticellite, and sodalite. Two voids found in *Al-2* (FoB) contain secondary larnite (Ca_2SiO_4) intergrowth with wollastonite and calcite with inclusions of wollastonite and monticellite.

Secondary minerals inside and outside fine-grained rims around CAIs: Fine-grained rims around Allende CAIs consist mainly of lath-shaped ferroan olivine and nepheline-ferroan olivine intergrowths; the latter are much more abundant than in the neighboring matrix. The rims are typically surrounded by a discontinuous layer of closely intergrown Ca-Fe-rich silicates – salite-hedenbergite pyroxenes, andradite, and wollastonite.

Oxygen Isotopes: Oxygen isotopic compositions of primary and secondary minerals in *TS21* (B1), *TS31* (B2), *Al-2* (FoB), and *100* (C) are shown in Fig. 2. Like in most Allende CAIs, primary melilite and anorthite in these inclusions are ^{16}O-depleted relative to spinel and Al,Ti-diopside having solar-like $\Delta^{17}O$. Most analyses of secondary grossular, wollastonite, monticellite, Na-melilite, sodalite, anorthite, dmisteinbergite, andradite, and calcite in Type B and FoB CAIs plot near the terrestrial fractionation line with $\Delta^{17}O$ of ~ –4 to –2‰ and relatively small range of $\delta^{18}O$ (~0 to 10‰). Grossular and forsterite in Type C CAI *100* have more ^{16}O-rich compositions ($\Delta^{17}O$ ~ –16 to –2‰ and –16 to –11‰, respectively) and on a three-isotope oxygen diagram plot approximately along the CCAM line. Anorthite grains in this CAI show a similar range of $\Delta^{17}O$ (from ~ –14 to ~ –4‰), whereas melilite grains are more ^{16}O-depleted ($\Delta^{17}O$ ~ –5 to –0‰).

Discussion: We have previously demonstrated that (*i*) coarse-grained grossular replacing melilite in the Allende igneous CAIs show no evidence for *in situ* decay of ^{26}Al, and (*ii*) resolvable excesses of ^{26}Mg* observed in Mg-rich grossular in veins crosscutting gehlenitic melilite mantles of Type B1 CAIs were inherited from melilite [10]. We conclude that Allende CAIs experienced open-system

metasomatic alteration, possibly multistage, in the presence of aqueous fluid with $\Delta^{17}O$ of ~ –2‰ on the CV parent asteroid > 3 Myr after their crystallization [10]. Calcium, Si, Mg, Na, Cl, Fe, and even Al were mobile during the alteration. The alteration resulted in formation of diverse secondary mineral assemblages controlled largely by the primary mineralogy and mineral chemistry of the host CAIs as well as chemistry of the fluid. A relatively small range of $\delta^{18}O$ among secondary minerals, compared to those of aqueously formed magnetite and carbonates in CR, CM, and CI chondrites [11], suggests the alteration occurred at higher temperature, most likely above 300°C. $\Delta^{17}O$ of most secondary minerals cluster around –4 to –2‰, which are close to the typical $\Delta^{17}O$ of primary melilite and anorthite of the Allende CAIs. Grossular and forsterite in Type C CAI *100* are significantly ^{16}O-enriched relative to melilite they replace. We infer that O-isotope exchange in the Allende CAIs could have started before and continued during and after formation of the secondary minerals.

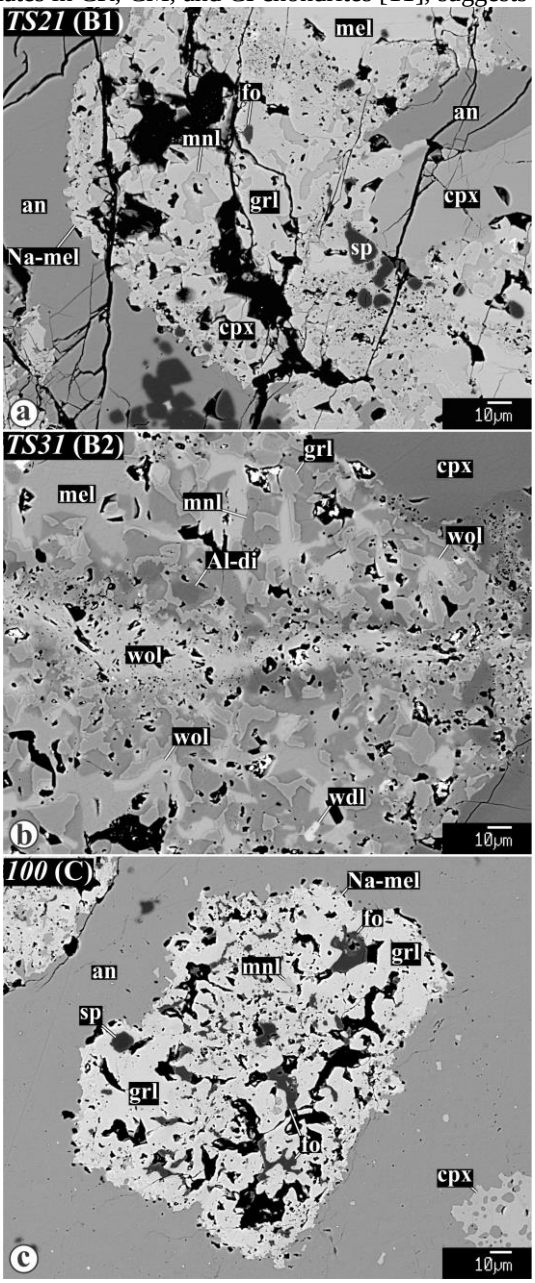

Fig. 1. BSE images of secondary minerals replacing melilite grains in the Allende CAIs (a) *TS21* (B1), (b) *TS31* (B2), and (c) *100* (C). For mineral abbreviations see Fig. 2.

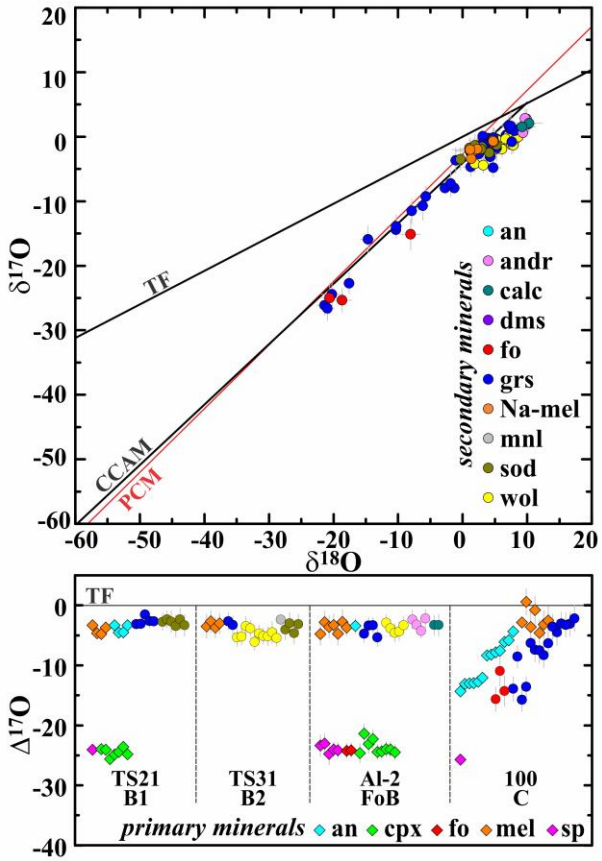

Fig. 2. (a) $\delta^{17}O$ *vs.* $\delta^{18}O$ and (b) $\Delta^{17}O$ of primary (circles) and secondary(diamonds) minerals in coarse-grained igneous CAIs *TS21* (B1), *TS31* (B2), *Al-2* (FoB) and *100* (Type C) from Allende (CV3.6). For clarity only $\Delta^{17}O$ of primary CAI minerals are plotted. an = anorthite; andr = andradite; calc = calcite; cpx = Al,Ti-diopside; dms = dmisteinbergite; fo = forsterite; grs = grossular; mel = melilite; mnl = monticellite; Na-mel = Na-rich melilite; sod = sodalite; sp = spinel; wol = wollastonite. CCAM = carbonaceous chondrite anhydrous mineral line; PCM = primitive chondrule mineral line [8]; TF = terrestrial fractionation line. Data for dmisteinbergite and anorthite are from [9].

References: [1] Krot A. et al. (1998) *MAPS 33*, 1065. [2] Fagan T. et al. (2007) *MAPS 42*, 1221. [3] Ushikubo T. et al. (2007) *MAPS 42*, 1267. [4] Brearley A. and Krot A. (2012) In *Metasomatism and the Chemical Transformation of Rock*, Springer-Verlag, 659–789. [5] Krot A. (2019) *MAPS 54*, 1647. [6] Nagashima K. et al. (2020) *LPSC 51*, #1719. [7] MacPherson G. (2014) In *Treatise on Geochemistry*, 139. [8] Ushikubo T. et al. (2012) *GCA 90*, 242. [9] Fintor K. et al. (2014) *MAPS 49*, 812. [10] Krot A. et al. (2010) *LPSC 41*, #1406. [11] Krot A. et al. (2015) In *Asteroids IV*, 635–661.